Catena 244 (2024) 108257

Contents lists available at ScienceDirect

Catena

journal homepage: www.elsevier.com/locate/catena

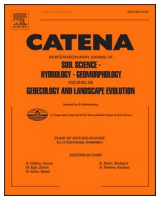

Extreme water repellency and loss of aggregate stability in heat-affected soils around the globe: Driving factors and their relationships

S. Negri [a,*], V. Arcenegui [b], J. Mataix-Solera [b], E. Bonifacio [a]

[a] University of Torino, Department of Agricultural, Forest and Food Sciences, Largo Braccini 2, 10095 Grugliasco, Italy
[b] Grupo de Edafología y Tecnologías del Medio Ambiente GETECMA, Department of Agrochemistry and Environment, University Miguel Hernández, Avda. de la Universidad s/n. 03202, Elche, Alicante, Spain

ARTICLE INFO

Keywords:
Thermal treatment
World biomes
Fire
Organic matter
Organo-mineral interactions

ABSTRACT

Wildfires impose deep modifications on soil organic matter (OM) and mineral phases, heavily affecting soil water repellency (WR) and aggregate stability (AS). The fallouts on soil fertility and erosion can be dramatic, and some soils might be more susceptible to these phenomena. Yet, no threshold values regarding specific soil properties or existing terrestrial ecosystems have been proposed.

In this study, thirty topsoils representative of a wide variety of biomes across the globe (from Savannah to Tropical, Mediterranean, Temperate and Boreal forests, and High elevation and latitude ecosystems) were subjected to a laboratory heating (at 200 and 300 °C) aimed at mimicking the behavior of a fire event. The samples were characterized for WR, AS, and the main drivers of organo-mineral interactions, such as pH, texture, abundance of iron (Fe) oxyhydroxides, organic C (OC) and inorganic C (IC) contents, and C/N ratio in the bulk soil and in the MACRO (2000 > Ø > 250 μm) and MICRO (Ø < 250 μm) size fractions. Water repellency, despite being highly variable among the samples, was always drastically lost when the soils were exposed to temperatures > 200 °C. At 200 °C, samples of Boreal and High latitude environments developed extreme WR values (>2000 s of infiltration time). The AS was also variable, and the same samples that experienced build-up of extreme WR showed a decrease in AS between 200 and 300 °C. The relationships between soil properties and heat-induced physical responses were non-linear, and two classification algorithms –Random Forest (RF) models- were used to identify the drivers of extreme WR development and AS loss.

Upon rising temperatures, acidic soils (pH<7) from cold and wet climates, with low clay content (<10 %) and a high proportion of poorly crystalline Fe oxides (Fe_{OXA}/Fe_{DCB} > 40 %), were far more prone to developing extreme WR. The loss of AS, on the other hand, was not induced in highly-developed Mediterranean, Tropical forest, and Savannah soils, where aggregation is mostly ruled by Fe oxyhydroxides and clay rather than by OM (ca. 50 g kg^{-1} of OC). In tight interlink with ecosystem resilience, this research clearly evidenced the vulnerability of specific biomes towards thermal-induced soil degradation.

1. Introduction

Wildfires are recognized as fundamental ecosystem shapers (Pickett and White, 2013) that have been impacting landscapes worldwide since the late Devonian (Glasspool et al., 2015). An average of 400 million hectares annually burn due to fire spread (Artés et al., 2019) and, of the estimated 7.20 billion hectares of fire-affected lands (over the 2001–2018 period), the largest areas belong to the African continent (over 65 % of the total burned surface). In decreasing order, we then find Oceania (ca. 12 % of the total area), America (10 %) and Europe (3.5 %) (FAO, 2020). The ongoing climate change is expected to favor large wildfires, with higher frequency and intensity (Bowman et al., 2009). Projections for future years forecast even more frequent and disruptive events (Jolly et al., 2015), both at global scale and in specific regions, like the Mediterranean basin, South-East Australia, South and North America (Bowman et al., 2020). In particular, a northward migration of fires in high latitude tundra-like environments has been foreseen (Chen et al., 2021).

Detrimental effects on soil physical integrity are frequently observed, since soil water repellency (WR) (Varela et al., 2010) and aggregation can be heavily impacted by fire occurrence (Mataix-Solera et al., 2011).

Water repellent soils are characterized by a limited water infiltration

* Corresponding author.
E-mail address: sara.negri@unito.it (S. Negri).

https://doi.org/10.1016/j.catena.2024.108257
Received 30 November 2023; Received in revised form 5 July 2024; Accepted 17 July 2024
0341-8162/© 2024 The Author(s). Published by Elsevier B.V. This is an open access article under the CC BY license (http://creativecommons.org/licenses/by/4.0/).

capacity, and may be so even in an unheated condition (Bisdom et al., 1993). In heated soils, WR can increase as the incomplete OM combustion leads to an enrichment in hydrophobic substances (Shakesby and Doerr, 2006) that condense as coatings on mineral particles (DeBano, 2000b). Cases of extreme soil WR have been reported both in lab-heating experiments (Araya et al., 2016; Atanassova and Doerr, 2011) and high-severity wildfires (Ferreira et al., 2005). The extent of heat-induced soil WR is primarily ruled by OM content and composition (Malkinson and Wittenberg, 2011), and the presence of some specific vegetation types (e.g., eucalypts and pines) that can trigger a great soil hydrophobicity (Hubbert et al., 2006; Zavala et al., 2014). In parallel, a coarse texture usually leads to high WR values due to an efficient OM coating effect (Mataix-Solera et al., 2014; Scott, 2000). When OM content is not enough to saturate mineral surfaces, the accessibility of clay surfaces (Doerr et al., 2000) or iron (Fe) oxy-hydroxides (Negri et al., 2021) may boost the soil hydrophobic character.

Soil aggregates are autonomous elements of soil structure (Fedotov et al., 2006), with a relatively stable association of mineral and organic phases guaranteed by physico-chemical-biological processes (Tisdall and Oades, 1982). Soil aggregate stability (AS) can either increase or decrease as a consequence of fire and laboratory heating (Arcenegui et al., 2008; García-Corona et al., 2004; Zavala et al., 2010) or experience no detectable variation (Llovet et al., 2009; Mataix-Solera et al., 2002). This variable behavior depends primarily on the influence of rising temperatures (Ts) on the main aggregate binding agents. Some studies have deemed OM as the dominant binding factor in many soils (Badía and Martí, 2003; Zavala et al., 2010), which are then expected to lose cohesiveness at high T (Girona-García et al., 2018). At the same time, heat-induced re-crystallization of Fe and aluminum (Al) oxides and presence of abundant clay contents may lead to greater AS at higher Ts (Giovannini and Lucchesi, 1997; Guerrero et al., 2001; Jordán et al., 2011).

The abundance and composition of both the mineral and the organic phase are highly variable worldwide, as they arise from pedogenic processes and local factors. Soils with different traits may then non-univocally respond to fire occurrence (Pellegrini et al., 2022). However, since different methods and techniques have been employed to evaluate soil WR and AS in connection to a drastic increase in soil temperatures, a comprehensive understanding targeting multiple environments at once is up-to-day lacking. We don't know how different soils would respond to fire.

This open question is pressing, considering that fire regimes are nowadays changing due to direct and indirect human actions. In addition to climate change, widespread land abandonment has caused shrub encroachment and forest spread in once-populated rural areas (Komac et al., 2013; Mantero et al., 2020), inducing greater flammability risks (Caballero et al., 2011).

For all these reasons, we gathered topsoils developed in diverse natural ecosystems and subjected them to a uniform lab-heating. Similar heating experiments are widely adopted both with combustion tunnels (Badía-Villas et al., 2014; Merino et al., 2018) and muffle furnaces (Araya et al., 2017) to mimic the behavior of different fire typologies or intensities on soil. We hypothesized that the response to heating would vary in soils of diverse ecosystems. Specifically, we aimed at:

i) Following the changes occurring with heating in soil chemical properties, WR and aggregation;
ii) identifying factors responsible for insurgence of extreme WR at high T, and providing useful threshold values;
iii) identifying factors responsible for loss of AS at high T, and providing useful threshold values

in a T-range realistically triggered in the topsoil by forest fires.

2. Materials and methods

2.1. Soil samples and heating treatment

Soil samples belonging to highly different environments around the globe were employed (Fig. 1). The dataset consists of surface horizons (A or E horizons) that embody a good –although not exhaustive– variability of soils at the world scale, as 7 of the 12 USDA soil orders are present (Soil Survey Staff, 1999). These samples developed under various vegetation covers and in different climates (for detailed samples description see Supplementary Information, Table S1), and are representative of i) High elevation/latitudes ecosystems (HEL), ii) Boreal (BOR), iii) Temperate (TEM), iv) Mediterranean (MED), v) Tropical (TRO) forests and vi) Savannah (SAV) environments.

The samples of HEL biome were collected under Andean tundra-like grassland, Magellanic forest and Scrub desert. They comprised topsoils developed in alpine/polar climates (ET, according to Koeppen classification, in the southern hemisphere) (Table S1). They were Entisols belonging to transition zones close to cold deserts and tundra-like vegetation, with dominance of tundra-like grasslands and shrubs (Mataix-Solera et al., 2021). The BOR biome was represented by soils of continental D climates (Dfb and Dfc). They were mainly Alfisols with a cryic soil temperature regime and Spodosols on granite and granodiorite with no limitation to water movements. The selected soils of the TEM biome (Cfb, Csb, Cfc climates) included Entisols, Inceptisols and Mollisols (Falsone et al., 2012). In the MED environment (Csa climate), non-zonal Entisols were collected in erosion-prone sites, and a typic Terra Rossa (Rhodoxeralf) was also chosen (Arcenegui et al., 2007). The soils belonging to the TRO formation (Cfa, humid subtropical climate) are represented by an Oxisol as well as by a non-zonal Inceptisol. The soils of SAV environments (Aw and BSh climates) covered a wide range of pedogenic evolution, from the Entisols of southern African desert borders to the Ultisols of Mali. Overall, conifers dominated both in Boreal and Mediterranean soils, while broad-leaved trees characterized Savannahs and Temperate forests.

The samples were air-dried, sieved (2 mm) and stored at room temperature (RT) until laboratory analysis. Each sample (BULK samples) was divided into four homogeneous subsamples. One was kept at RT, while 10 g of each subsample were placed in large ceramic crucibles (resulting thickness of ca. 1 cm) and heated for 30 min in a muffle furnace at 200 and 300 °C. The 30 min heating time and the Ts tested were selected in agreement with recent studies (Araya et al., 2016, 2017; Varela et al., 2010). Also, we focused on these temperatures as existing literature reports the development of maximum water repellency around 200 °C and its loss above this temperature (Negri et al., 2021), and because aggregates experience transformations in this exact temperature-range (DeBano, 2000b; Mataix-Solera et al., 2011), which corresponds to low-moderate fire intensity (Janzen and Tobin-Janzen, 2008).

2.2. Soil water repellency and aggregates characterization

Soil water repellency was evaluated by the Water Drop Penetration Time (WDPT) test on unheated and heated samples. To ensure comparability of the results, WDPT was measured after keeping the samples in a climatic chamber for 24 h. Room relative humidity was verified to be always around 30–50 % during WDPT testing (Beatty and Smith, 2010; Diehl et al., 2010; Papierowska et al., 2018). We employed a standard 0.1 mL dropper and recorded WDPT up to over 4000 s. Four drops of distilled water were placed on the soil flattened surface.

Each BULK soil sample (at RT, 200 °C and 300 °C) was dry sieved and divided in MICRO (Ø<250 μm) and MACRO (2000>Ø>250 μm) size fractions. The relative contributions of the two fractions to the BULK soil was then calculated (MICRO and MACRO contents, %). Following Roldán et al. (1996), the MACRO fraction was placed on a 250 μm sieve and subjected to a rainfall simulation (height of 1 m, impact energy of

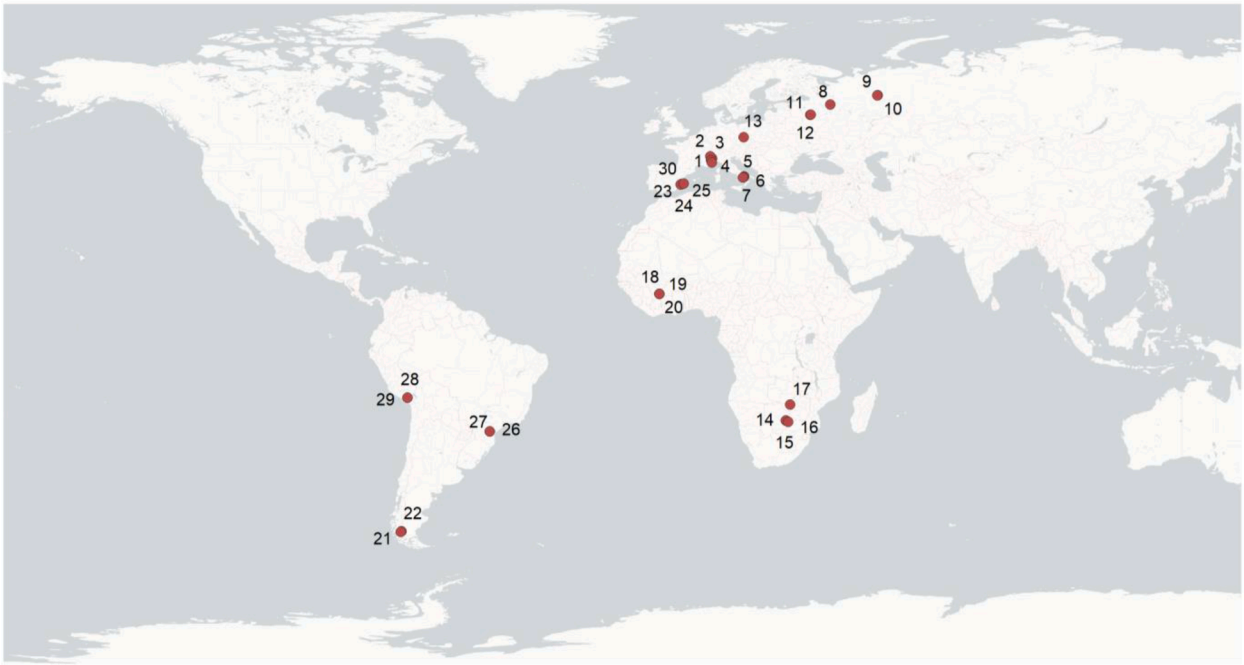

Fig. 1. Localization of samples across the globe.

270 J/m^{-2}(−|−)), which caused the breakdown of the weakest aggregates (WA). The soil remaining on the sieve was oven-dried, weighed and the weight of coarse particles (Ø > 250 μm) was subtracted to determine the proportion of resistant aggregates (RA, %). The AS was calculated as follows (Eq. (1)):

$$AS = \frac{RA}{(RA + WA)} \times 100(\%) \quad (1)$$

Therefore, RA refers to the proportion of aggregates that resist the rainfall (i.e., g RA 100 g^{-1} of soil), while AS refers to the proportion of resisting aggregates respect to the total amount of aggregates present in the sample.

2.3. Soil physical and chemical analyses

Soil particle size distribution (PSD) was analyzed by the pipette method after dispersion with Na-hexametaphosphate (Gee and Bauder, 1986). Size classes were classified as: coarse sand (2000 > Ø > 200 μm), fine sand (200 > Ø > 50 μm), coarse silt (50 > Ø > 20 μm), fine silt (20 > Ø > 2 μm) and clay (Ø < 2 μm). Soil pH was evaluated potentiometrically in a 1:2.5 soil:deionized water suspension after 2 h shaking (Gee and Or, 2002).

Total soil C and total N were determined by dry combustion (Unicube CHNS Analyzer, Elementar, Langenselbold, Hesse, Germany), and organic C (OC) was determined again after inorganic C (IC) removal by HCl (Harris et al., 2001). These analyses were performed on BULK (OC, IC, N, C/N), MACRO (OC_M, IC_M, N_M, C_M/N_M), and MICRO (OC_m, IC_m, N_m, C_m/N_m) soil fractions. We then calculated OC_M/OC_m. The OC losses observed at high temperature (at 300 °C) were expressed in terms of concentrations (i.e., g OC kg^{-1} of soil or soil fraction), and were also expressed as relative losses with respect to the initial (25 °C) OC concentration. The relative OC losses (Norm OC LOSS) were calculated for the BULK samples, as well as for MACRO and MICRO fractions.

On BULK samples, total pedogenic Fe oxides were extracted with a Na-dithionite-citrate-bicarbonate (DCB) solution (Mehra and Jackson, 1958). Acid ammonium oxalate (OXA) solution in the dark (Schwertmann, 1964) was employed to assess the contribution of poorly crystalline Fe oxides, and the pool of Fe associated with OM was isolated with a Na-pyrophosphate (PYRO) solution (Loeppert, 1996). Fe content in the extracts was determined by AAS (Thermo Scientific iCE 3000, Cambridge, United Kingdom). The different Fe pools were addressed as Fe_{DCB}, Fe_{OXA} and Fe_{PYRO}, and Fe_{OXA}/FeD_{CB} and Fe_{PYRO}/Fe_{DCB} were derived. The Fe_{DCB} was also measured in the MACRO and MICRO size fractions ($Fe_{DCB\ M}$ and $Fe_{DCB\ m}$, respectively), and their ratio was calculated ($Fe_{DCB\ M}/Fe_{DCB\ m}$).

2.4. Statistical analyses

RStudio (R version 4.2.3) was used for statistical purposes. The soil properties were grouped according to biome of belonging, and graphically presented with boxplots, polar plots and stacked bar-plots. Shapiro-Wilk's and Levene's tests were applied to inspect normality and homoscedasticity of the data. Non-normal data were log-transformed. One-way ANOVA was used to test differences in mean values between groups (threshold for statistical significance set at 0.05), and Tukey-HSD test was applied for post hoc pairwise comparisons. When describing the evolution of soil properties alongside the T-kinetic (25–200-300 °C), linear mixed models were used to test differences according to biome of belonging and temperature (and their interaction). When present, autocorrelation was considered within the model structure, and choice of the best model was operated on the basis of Akaike's information criterion (AIC).

To identify the driving factors ruling extreme WR and loss of AS at high temperature, the soil properties regulating soils WR and AS expression at various temperatures were screened by inspecting correlation matrices (computed with the use of the non-parametric rank-based Spearman method) and Principal Component Analysis (PCA) biplots. The matrices were scaled and centered prior to generating biplots.

To predict cases of extreme WR and loss of AS at high T, samples were assigned a binary categorical class: 0/1 for insurgence of extreme WR, 0/1 for occurrence of AS loss. After having observed the structure of the dataset, we assigned the binary categorical class of extreme WR (1) to the samples that developed WDPT>2000 s at 200 °C, and the class of AS loss (1) to the samples that lost more than 10 % of the initial AS when shifting from 200 to 300 °C.

Two distinct Random Forest (RF) models (Breiman, 2001) in

classification mode were then computed: one to predict the insurgence of extreme WR, and another one to predict the occurrence of AS loss at high Ts. The data was partitioned in train and test data, and the covariates in use included the soil properties strongly correlated to either WR or AS expression (previously screened with correlograms and PCA), and environmental variables like site average annual temperature (av.T., °C), precipitation (mm year^{-1}), latitude (°), elevation (m a.s.l), soil type, vegetation type. The Aridity Index (AI) by De Martonne (1926) was also calculated (Equation (2):

$$AI = \frac{precipitation}{av.T + 10} \quad (2)$$

The climatic data (average annual precipitation, average annual temperature) of each site was derived by Karger et al. (2017), available at Climate Diagrams (mapresso.com). Higher AI values are related to abundant precipitations and lower average annual temperature (av.T). The performance of the models was assessed with the out-of-bag estimate by tuning the number of trees. Partial dependence plots were drawn for the most relevant driving factors (Ehrlinger, 2016).

3. Results

3.1. Bulk soil characteristics, and changes in chemical properties after heating

Soils of TRO and SAV biomes were characterized by a higher abundance of coarse sand ($p < 0.01$, Fig. 2a and Table S2). Clay was conversely significantly higher in soils of MED environments when compared to BOR, HEL and SAV soils ($p < 0.01$). The IC was abundant in MED soils, and was present in TEM soils, while it was not present in the other samples (Fig. 2b). At RT, the pH was significantly higher in SAV and MED samples ($p < 0.05$), with the absolute lowermost values in BOR samples (Table 1). Also, at RT the OC content was highly inhomogeneous among the soils (average = 41.5 g kg^{-1}, st. dev. = 38.9 g kg^{-1}), with the lowest values in SAV sites ($p < 0.01$, Table1). Together with little OM content, the SAV samples also displayed extremely low C/N values, while BOR and MED presented the highest ones ($p < 0.01$, Table 1). The soils of TEM environments were significantly richer in Fe_{DCB}, while lower values occurred for HEL, BOR and SAV samples ($p < 0.01$, Table 1 at 25 °C). The degree of Fe oxides crystallinity followed a biome-related gradient, with higher Fe_{OXA}/Fe_{DCB} values in BOR and HEL samples ($p < 0.001$). At RT, the proportion of Fe-OM pool (Fe_{PYRO}/Fe_{DCB}) accounted for significantly higher values in BOR soils respect to SAV and HEL soils ($p < 0.05$), with intermediate values for the other biomes.

Variations in soil chemical properties were visible upon heating

Table 1
Mean pH values, OC content (g kg^{-1}), C/N ratio and iron forms –Fe_{DCB} (g kg^{-1}), Fe_{OXA}/Fe_{DCB} (%), Fe_{PYRO}/Fe_{DCB} (%)- in the soils belonging to different biomes at RT condition (25 °C), 200 and 300 °C. Values in parentheses are standard deviations. Lowercase letters indicate statistically significant differences among biomes within each selected temperature; uppercase letters, if present, indicate differences according to the temperature:biome interaction effect.

T	Biome	pH	OC (g kg^{-1})	C/N	Fe_{DCB} (g kg^{-1})	Fe_{OXA}/Fe_{DCB} (%)	Fe_{PYRO}/Fe_{DCB} (%)
25	HEL	5.9 ^{ab}	57.7 ^{a}	14 ^{ab}	4.2^{b}	38.8 ^{ab}	15.1^{b}
		(±0.2)	(±10.2)	(±2)	(±3.4)	(±10.4)	(±6.5)
	BOR	4.5^{b}	35.7 ^{a}	19 ^{a}	4.0^{b}	59.9 ^{a}	52.3 ^{a}
		(±1.2)	(±33.6)	(±7)	(±3.1)	(±11.3)	(±22.0)
	TEM	6.1 ^{ab}	59.3 ^{a}	13 ^{ab}	14.7 ^{a}	29.0 ^{bc}	22.7 ^{ab}
		(±1.5)	(±28.7)	(±2)	(±5.3)	(±14.2)	(±23.6)
	MED	7.2 ^{a}	83.4 ^{a}	17 ^{a}	8.6 ^{ab}	20.7 ^{bcd}	25.7 ^{ab}
		(±1.8)	(±55.8)	(±1)	(±9.6)	(±19.0)	(±23.0)
	TRO	5.6 ^{ab}	20.5 ^{ab}	13 ^{ab}	11.9 ^{ab}	6.7^{cd}	34.7 ^{ab}
		(±0.1)	(±1.6)	(±1)	(±9.9)	(±2.6)	(±31.0)
	SAV	6.4 ^{a}	6.4^{b}	10^{b}	3.3^{b}	6.1 ^{d}	15.6^{b}
		(±0.2)	(±2.6)	(±2)	(±1.7)	(±3.4)	(±13.3)
200	HEL	5.9 ^{ab}	52.3 ^{a}	12	3.7^{b}	51.1 ^{ab}	20.8 ^{ab}
		(±1.0)	(±6.6)	(±2)	(±3.3)	(±9.4)	(±7.3)
	BOR	4.5^{b}	31.5 ^{a}	14	4.0^{b}	61.5 ^{a}	52.3 ^{a}
		(±0.8)	(±32.2)	(±3)	(±3.3)	(±18.6)	(±28.0)
	TEM	6.5 ^{a}	50.6 ^{a}	11	16.0 ^{a}	29.7 ^{bc}	19.1^{b}
		(±1.1)	(±20.5)	(±2)	(±5.4)	(±15.0)	(±15.6)
	MED	7.3 ^{a}	65.6 ^{a}	14	8.9 ^{ab}	17.7^{c}	15.7^{b}
		(±1.7)	(±43.6)	(±2)	(±8.8)	(±16.8)	(±12.2)
	TRO	5.2 ^{ab}	17.4 ^{ab}	12	9.6 ^{ab}	10.3^{c}	30.1 ^{ab}
		(±0.4)	(±2.1)	(±1)	(±9.1)	(±7.2)	(±25.2)
	SAV	5.8 ^{ab}	6.1^{b}	10	3.0^{b}	9.0^{c}	19.6^{b}
		(±0.3)	(±2.4)	(±2)	(±1.6)	(±6.2)	(±17.0)
300	HEL	8.1 ^{a}	19.1 ^{ab}	6	4.2^{b}	47.3 ^{a}	21.2 ^{a}
		(±0.6)	(±5.4)	(±1)	(±3.2)	(±7.2)	(±6.3)
	BOR	5.7^{b}	10.8 ^{bc}	7	4.6^{b}	51.1 ^{a}	26.5 ^{a}
		(±1.9)	(±11.5)	(±2)	(±3.1)	(±17.0)	(±23.0)
	TEM	7.7 ^{a}	22.9 ^{ab}	6	15.2 ^{a}	38.6 ^{a}	8.7 ^{ab}
		(±1.6)	(±11.7)	(±1)	(±3.9)	(±17.5)	(±4.4)
	MED	9.1 ^{a}	38.1 ^{a}	10	8.8 ^{ab}	26.3 ^{ab}	8.4 ^{ab}
		(±0.7)	(±34.5)	(±4)	(±9.3)	(±22.2)	(±5.6)
	TRO	6.4 ^{ab}	7.7 ^{bc}	6	11.3 ^{ab}	8.0^{b}	7.7^{b}
		(±0.4)	(±1.8)	(±1)	(±9.4)	(±4.2)	(±5.2)
	SAV	7.4 ^{ab}	3.2^{c}	6	3.5^{b}	8.2^{b}	7.8^{b}
		(±0.4)	(±1.6)	(±1)	(±1.8)	(±4.4)	(±5.6)

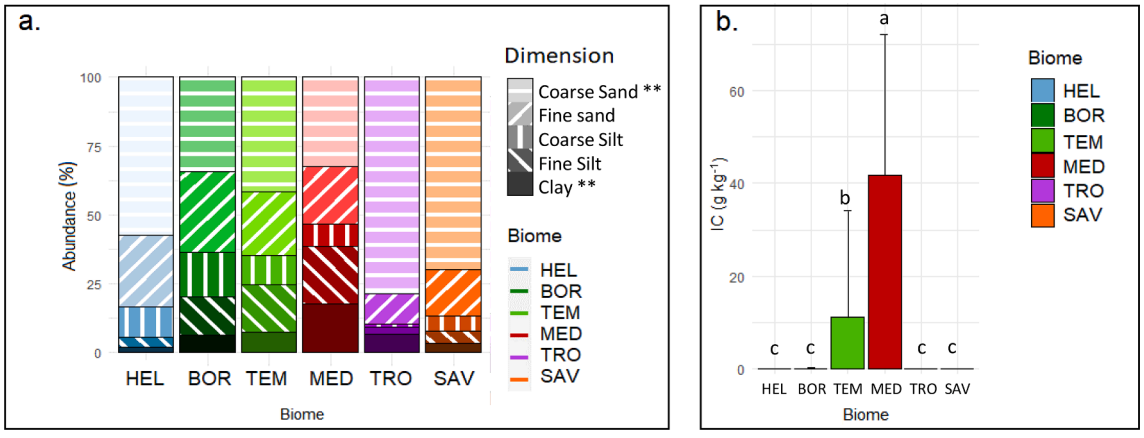

Fig. 2. Main bulk soil properties at RT condition: PSD classes (pattern according to particle size dimension); b. bar-plot with IC content (g kg^{-1}). Color-code according to biome of belonging. Stars (*) and letters indicate statistically significant differences in mean values.

(Table 1). All samples had lower OC contents at 300 °C respect to room temperature and 200 °C ($p < 0.001$), without any significant interaction of temperature and biome of belonging ($p > 0.05$ for T:biome effect). At 300 °C, the amount of OC lost by the bulk soil in proportion to the OC at RT condition (Norm OC LOSS) was on average 60.5 % (st. dev. = 11.5 %), and was significantly lower in SAV samples respect to BOR and HEL samples ($p < 0.001$, Fig. S1). The OC losses induced by the high temperature were coupled with significantly lower C/N values at 300 °C ($p < 0.001$, and $p > 0.05$ for the T:biome interaction, Table 1), as well as significantly higher pH values at 300 °C respect to room temperature and 200 °C ($p < 0.001$, and $p > 0.05$ for the T:biome interaction effect). The high temperatures also triggered a decrease in the Fe-OM pool, with significantly lower Fe_{PYRO} contents at 300 °C ($p < 0.01$, and $p > 0.05$ for the T:biome interaction, Table 1). In parallel, heat hardly affected the mineral phases present in the soils. The Fe_{DCB} was not altered by the rising Ts ($p > 0.05$), nor was the Fe_{OXA}/Fe_{DCB} ratio ($p > 0.05$).

3.2. Properties of the aggregate fractions

The MACRO fraction was more abundant in the MED and TRO soils, and significantly lower ($p < 0.001$) in samples of SAV and HEL biomes (Fig. 3a and Table S3). The SAV samples were also the ones with the lowest amount of OC_M ($p < 0.001$), less than 20 g kg^{-1}. The distribution of OC content in the MACRO and MICRO fractions (OC_M/OC_m) also differed, being the MACRO fraction OC-richer in samples of HEL, BOR and MED biomes (Fig. 3a). The absolute lowermost OC_M/OC_m values corresponded to TRO soils ($p < 0.05$, Fig. 3a), and the C/N values were always higher in the MACRO than in the MICRO size fraction ($p < 0.01$). The inorganic cements, IC_M and Fe_{DCB}, displayed trends similar to the bulk soil ($p < 0.01$ and $p < 0.05$, respectively), as shown in Fig. 3b. Pedogenic Fe oxides were mostly concentrated in the MICRO size fraction (average $Fe_{DCB\ M}/Fe_{DCB\ m} = 0.55$, st. dev. = 0.47), and there was no significant difference in $Fe_{DCB\ M}/Fe_{DCB\ m}$ on the basis of biome of belonging.

No significant change in the proportion of MACRO and MICRO fractions was detected upon heating the samples (Fig. S2, $p > 0.05$). The amount of OC lost at 300 °C was similar in the MICRO and MACRO fractions ($p > 0.05$), and the absolute lowest values corresponded to SAV samples ($p < 0.001$, Fig. 3c). Once these amounts were normalized to the OC content present at RT (Norm OC LOSS), a different scenario emerged (Fig. 3d). Greater relative OC losses occurred in the MACRO than in the MICRO size fraction ($p < 0.01$), and the differences were visible also among biomes. The lowermost proportional OC losses were recorded in case of the MED MACRO fraction (Fig. 3d).

3.3. Responses of water repellency and aggregate stability to heat

The WR and AS of these soils were variable already at the initial condition (Fig. 4a and 4d). At RT, the greatest WR as measured by WDPT was recorded in HEL samples (maximum infiltration times over 400 s, Fig. 4a), while SAV soils were extremely wettable ($p < 0.05$) and samples belonging to other biomes displayed an intermediate behavior. The samples belonging to the SAV biome also displayed the lowermost AS (Fig. 4d, $p < 0.005$), while soils of TRO, TEM and MED were characterized by average AS values above 80 %. The amount of resistant aggregates (RA) at RT did not follow the same biome-related trend as AS (Fig. 4g, $p < 0.001$). The SAV soils were an exception, showing very low RA values in addition to low AS. In TRO soils, the high AS was coupled

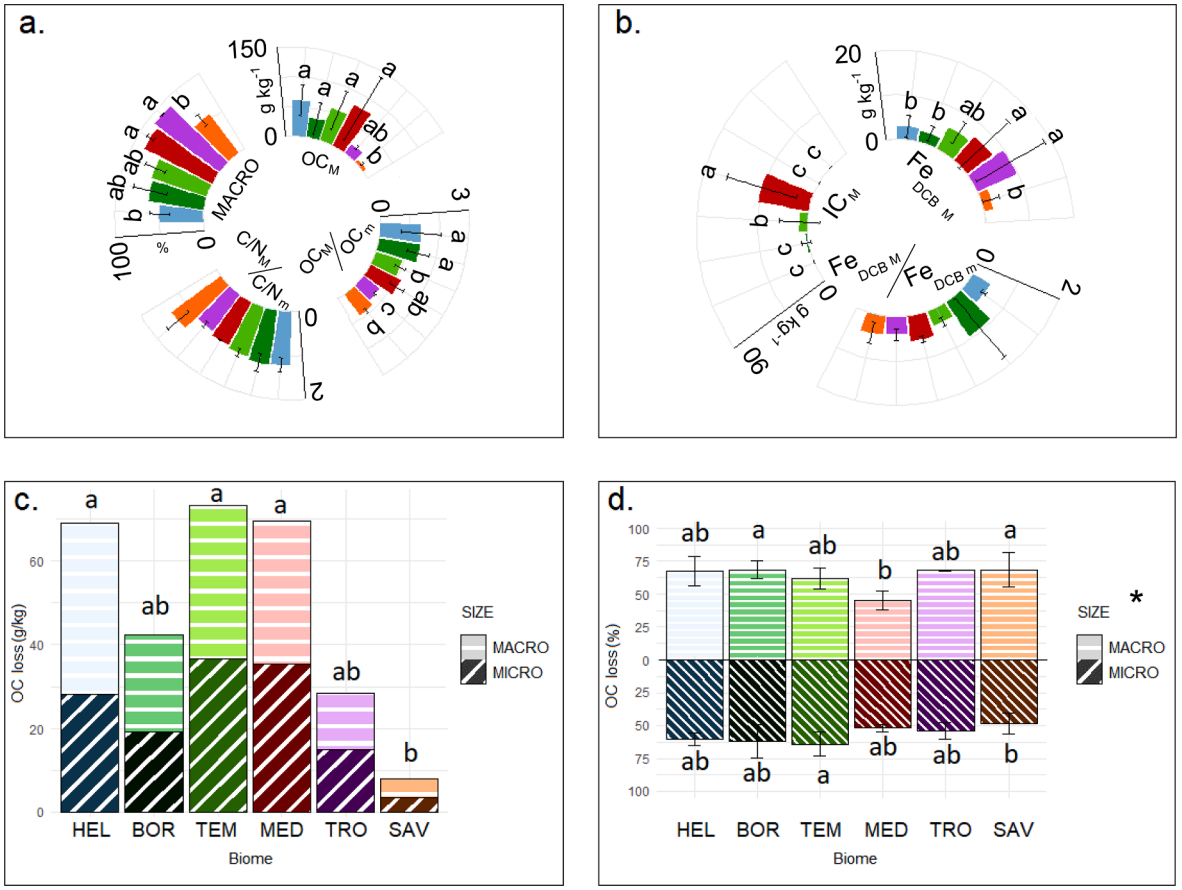

Fig. 3. Main properties of the soil size fractions. a. Polar plot with MACRO content (%), OC_M content (g kg^{-1}), OC_M/OC_m, $C/N_M/C/N_m$; b. polar plot with IC_M content (g kg^{-1}), $Fe_{DCB\ M}$ (g kg^{-1}), $Fe_{DCB\ M}/Fe_{DCB\ m}$; c. bar-plot with OC losses in soil size fractions (g kg^{-1}); d. bar-plot with Norm OC losses in soil size fractions (%). Color-code according to biome of belonging, pattern according to size fraction. Letters indicate statistically significant differences in mean values.

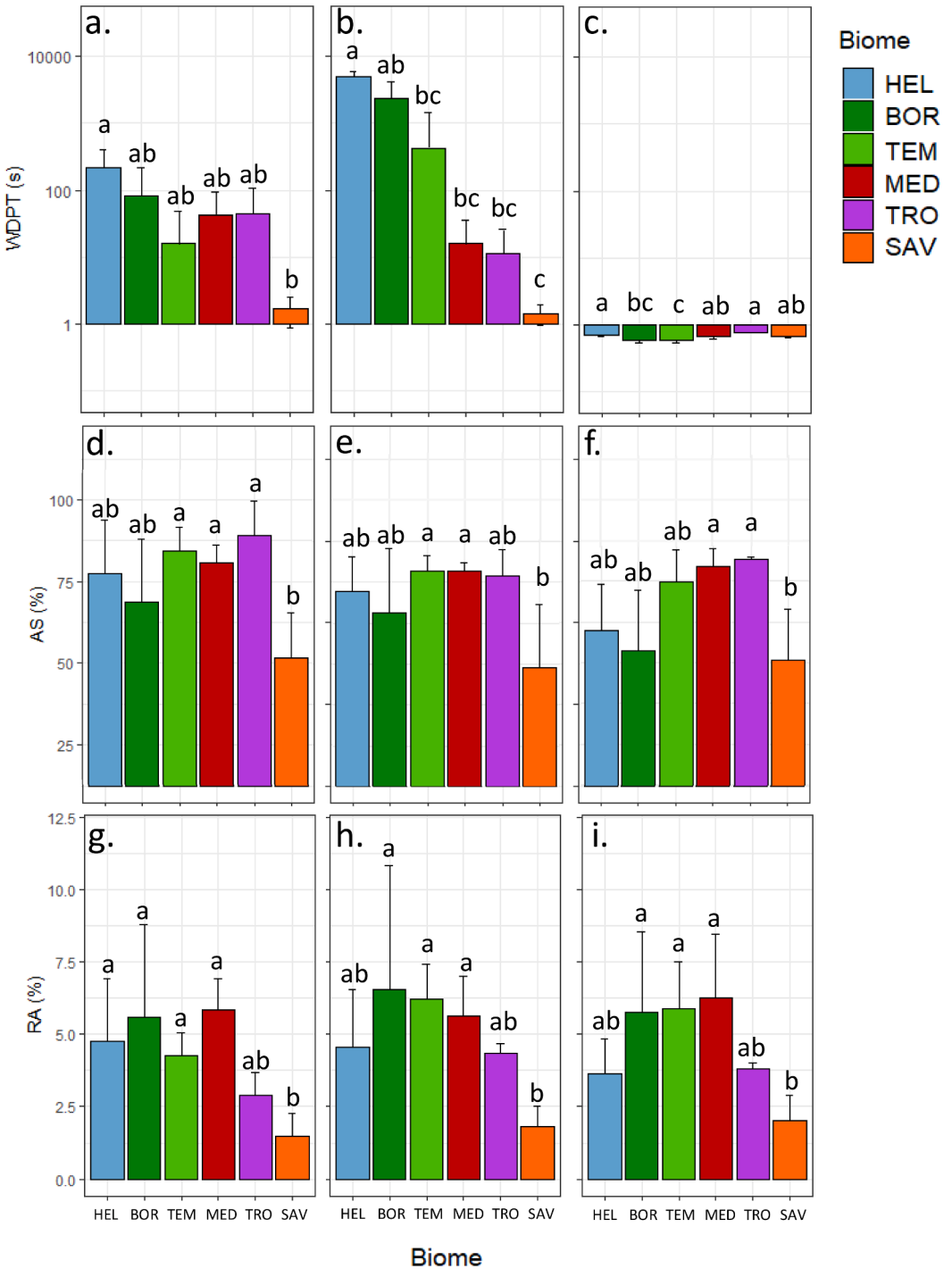

Fig. 4. Bar-plots with a. WDPT (s) at 25 °C; b. WDPT (s) at 200 °C; c. WDPT (s) at 300 °C; d. AS (%) at 25 °C; e. AS (%) at 200 °C; f. AS (%) at 300 °C; g. RA (%) at 25 °C; h. RA (%) at 200 °C; i. RA (%) at 300 °C. Color-code according to biome of belonging, letters indicate statistically significant differences in mean values.

with low RA values and, conversely, BOR soils were characterized by a remarkable amount of RA and intermediate AS values, similar to that of MED soils.

Heating significantly affected WR in the studied soils ($p < 0.001$). At 200 °C (Fig. 4b), a marked increase in WR occurred for samples belonging to HEL and BOR biomes (the same samples that presented high WR already at RT) and TEM, while SAV soils remained wettable alongside the whole T-kinetic. An intermediate behavior characterized the other samples (Fig. 4b), and a generalized flattening of infiltration times (with values < 1 s) was measured at temperatures of 300 °C (Fig. 4c). The loss of WR occurred for all the soils, regardless of the hydrophobicity displayed up to that temperature. The soils showing the biggest changes in WR between 25 and 300 °C are those belonging to the BOR and HEL biomes.

The responses of aggregates to heating are less straightforward. For BOR and TRO, the percentage of RA peaked at 200 °C, showing no clear trend in the other biomes (Fig. 4h and i). Conversely, AS showed a slight increase at 200 °C for soils of all biomes but TRO (Fig. 4e). After this threshold, a decrease in AS was visible for HEL, BOR and TEM, while AS continued to increase in the soils of MED, TRO and SAV (Fig. 4f). These heat-induced changes in AS were at the border of statistical significance ($p = 0.06$). In general, the soils that displayed extreme WR at 200 °C

(belonging to HEL and BOR biomes, Fig. 4b) also exhibited a decrease in AS from 200 to 300 °C.

3.4. Driving factors behind soil water repellency and aggregate stability expression

Soil WR was not strongly correlated to any of the investigated soil properties (Fig. 5), and only a moderate positive correlation with OC ($R = 0.394$, $p < 0.05$) and OC_M ($R = 0.419$, $p < 0.05$) emerged at RT. These relationships were lost at 200 °C ($R = 0.314$, $p > 0.05$ for OC; $R = 0.309$, $p > 0.05$ for OC_M), and WR resulted more closely related to abundance of poorly crystalline Fe oxides ($R = 0.517$, $p < 0.01$). No single obvious soil characteristic seems therefore appropriate to quantitatively follow the hydrophobic behavior of these widely differing soils.

When the problem was simplified by categorizing water repellency into development of extreme WR (i.e. WDPT>2000 s) or not, and the number of influencing variables was reduced through PCA (Supplementary Information, Fig. S3a), extreme WR was found to strictly associate with high Fe_{OXA}/Fe_{DCB}, low pH and Aridity Index (AI) values. Also, abundance of OC and different size fractions (clay and fine silt *vs.* sand) appeared as dominant factors explaining WR expression, but these factors were not able to discriminate between samples that showed/did not show extreme WR (Fig. S3a).

The negative contribution of sand fractions to aggregation parameters clearly emerged (Fig. 5): fine sand content was negatively and significantly correlated with AS at RT ($R = -0.572$, $p < 0.01$) and 300 °C ($R = -0.430$, $p < 0.05$), and was also was negatively and significantly correlated with MACRO abundance at all Ts ($R < -0.490$, $p < 0.05$). Coarse sand was negatively correlated to RA at all Ts ($R < -0.500$, $p < 0.01$). Positive and significant correlations were instead found between the clay fraction and aggregation parameters (MACRO and RA), and between Fe forms and aggregation (AS and RA, Fig. 5). In particular, Fe_{DCB} was weakly related to AS at 25 °C and 300 °C ($R>0.420$, $p < 0.05$), and the Fe_{OXA}/Fe_{DCB} was significantly and positively related to RA at 25 °C and 200 °C ($R>0.500$, $p < 0.01$). A positive relationship was also noted between OC and AS at RT ($R = 0.549$, $p < 0.01$). This relationship was strengthened at 200 °C ($R = 0.565$, $p < 0.01$) and, while WR was found to be more strongly related to OC_M rather than OC_m (as mentioned above), the situation was reversed in the case of AS (at 25 °C: $R = 0.474$, $p < 0.01$ for OC_M and $R = 0.571$, $p < 0.01$ for OC_m; at 200 °C: $R = 0.489$, $p < 0.01$ for OC_M and $R = 0.590$, $p < 0.01$ for OC_m).

Also in this case, when the loss of aggregate stability upon heating was considered −and the variables were reduced by PCA, the samples with a decrease in AS greater than 10 % from 200 to 300 °C were those primarily associated with high amounts of fine sand and high AI values, and low MACRO and OC contents (Fig. S3b). Other parameters that were deemed as fundamental are abundance of pedogenic Fe oxides (Fe_{DCB}) and specific size fractions (sand and silt, Fig. S3b). The discrimination between samples with weak and heat-resistant aggregates is less clear than for samples that develop or not extreme water repellency, as a large overlapping area in Fig. S3b exists both along the PC1 and the PC2 axes. All samples were topsoils and, therefore, OM is expected to always play a role in aggregation, in addition to some more site-specific factors. The combination of organic and inorganic binding agents might have masked some more marked behaviors, possibly mitigating the loss of aggregates upon heating.

The first RF model, built using the factors identified through PCA, revealed that soil pH is the main variable related to extreme WR (RF model output in Fig. 6a). Acidic topsoils (pH<7, Fig. 6b) with low clay contents (<10 %, second partial dependence plot in Fig. 6b) and Fe oxides with a poor crystalline structure (Fe_{OXA}/Fe_{DCB}>40 %, third partial dependence plot in Fig. 6b) were found to favor the development of high WR values. Also, high AI values (>75, fourth partial dependence plot in Fig. 6b) were associated with extreme WR. From the climatic point of view (AI index) it appears that the most sensitive soils are those characterized by temperatures and precipitation regimes that favor water availability for soil processes, leading to a decrease in pH. Soils of warmer and drier environments, conversely, appear less prone to develop extreme WR after heating.

The second RF model evidenced that the lack of the MACRO fraction is the main factor responsible for heat-induced AS loss (Fig. 7a and b). Apparently, the presence of MACRO aggregates in less than 50 % of the bulk soil sample (w/w %) will make the soil highly sensitive to detrimental effects (as visible in the first partial dependence plot of Fig. 7b). The AI was the second factor with explanatory power in Fig. 7a, and evidenced that soils in environments with AI>70 would struggle coping with fire occurrence (Fig. 7b). Aggregates were less affected by the increasing Ts in soils containing ca. 50 g kg^{-1} of OC (Fig. 7b), where particle-aggregation was mostly ruled by inorganic binding agents in the form of Fe-oxides (3rd partial dependence plot in Fig. 7b) and carbonates (IC, 7th factor in Fig. 7a). The soils where AS loss was least affected by the high Ts were those dominated by deciduous vegetation (Fig. S4b).

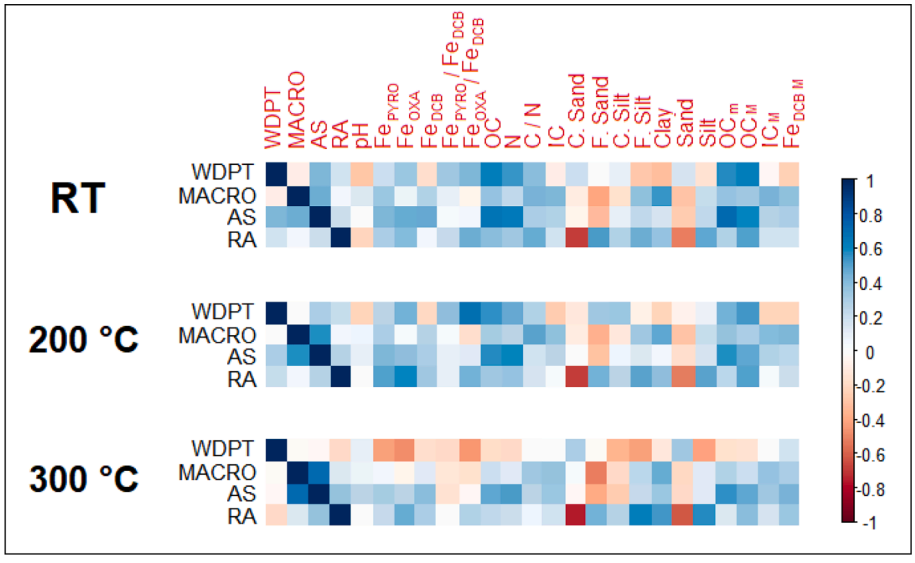

Fig. 5. Corrplot with red-to-blue colorbar (−1 to 1) at various temperatures (RT-200–300 °C).

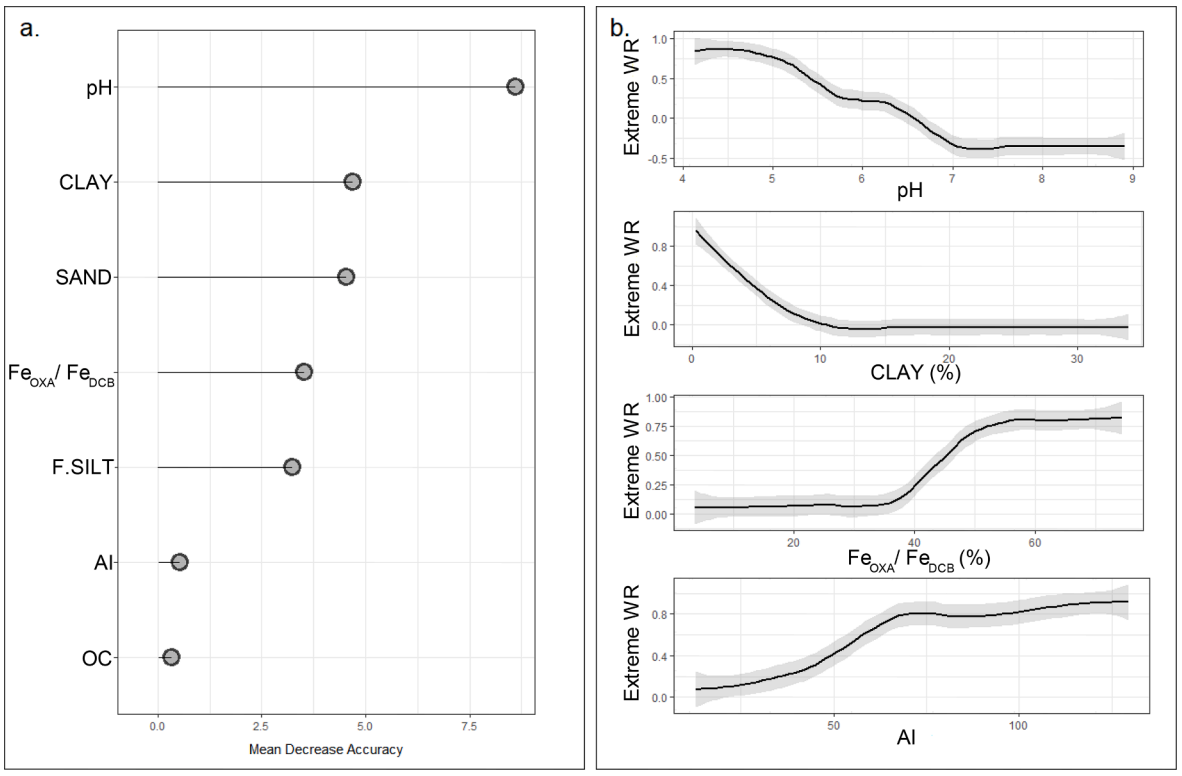

Fig. 6. A. accuracy plot of the main variables regulating extreme wr expression; b. partial dependance plots of selected variables.

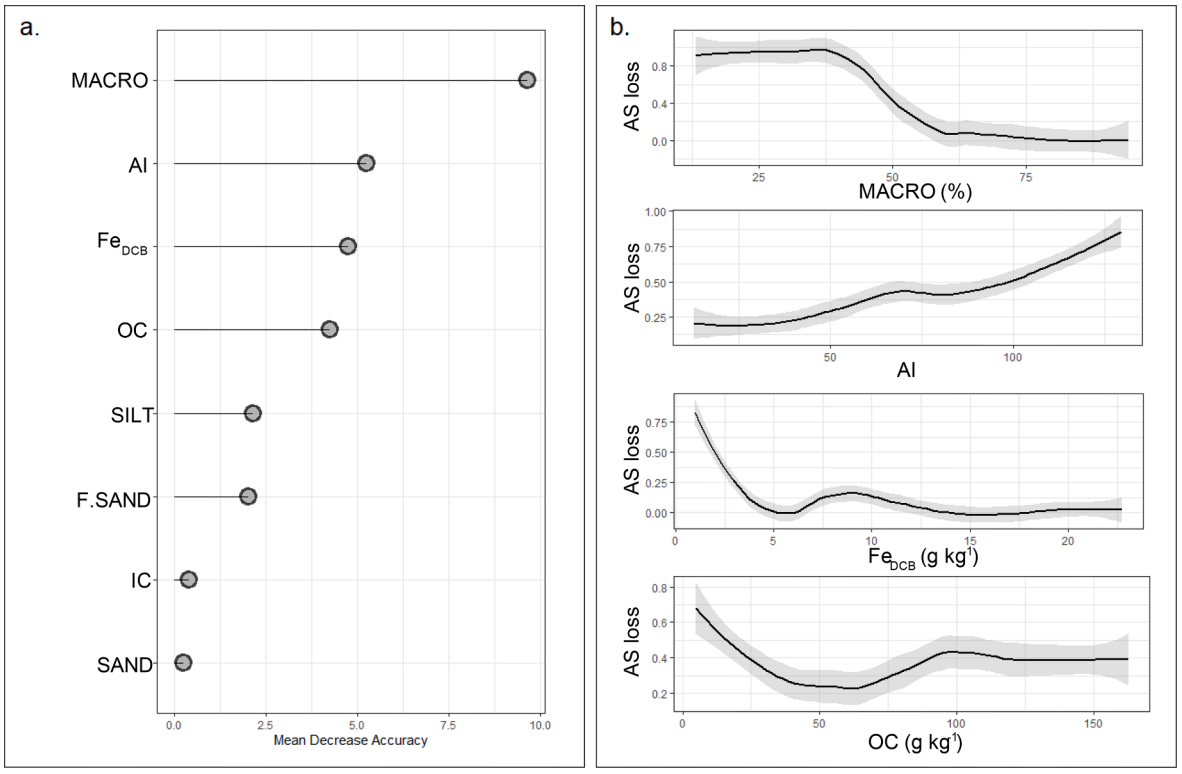

Fig. 7. A. accuracy plot of the main variables regulating as loss; b. partial dependance plots of selected variables.

4. Discussion

4.1. Soil variability and organo-mineral interactions at room temperature

Soil chemical properties were generally in line with the dominant pedogenic factors and processes that characterize the various biomes. The high C/N ratio in BOR well depicted the dominant conifer vegetation (Table1), the high pH in SAV and MED soils reflected the lower amount of water available for leaching in these environments, while the importance of poorly crystalline Fe forms in BOR (high Fe_{OXA}/Fe_{DCB} values in Table 1) is in line with the hampering of crystallization by OM and soil acidity (Borggaard, 1985).

As the dataset included non-zonal soils, site factors other than climate and vegetation have played a role in the development of soil characteristics. This is the case of the abundance of the coarse fraction in SAV soils (Fig. 2a), linked to the presence of sandstones and Kalahari sands as parent materials in soils from southern Africa (Bonifacio et al., 2006). The parent material is also the driver of the paucity of Spodosols in the boreal forests of Russia, where fluvioglacial fine sediments impede podzolization despite the presence of conifers (Bonifacio et al., 2009). The abundance of IC was expected in MED environments, but it is less obvious in soils from TEM beech stands. In this case, the calcareous parent material, along with a seepage position, allowed the precipitation of secondary carbonates and the development of a Mollisol (Catoni et al., 2016). The high content of OM in MED soils is not a feature typical of all soils in this environment (Andrés-Abellán et al., 2019), while the low-to-average OC contents in BOR samples are likely related to an abundant accumulation of OC in the forest floor (Hilli et al., 2010).

Since both the amount and the type of mineral surfaces available for OM sorption varied in the studied soils, we expected a complex and biome-specific interaction between these phases, which was confirmed by the only moderate positive correlation of water repellency with OC ($R = 0.394$, $p < 0.05$) and OC_M ($R = 0.419$, $p < 0.05$). Our results on WR agree with published data corresponding to soils of various ecosystems and, for once, strongly water repellent (600 s > WDPT > 60 s) and extremely water repellent (WDPT > 3600 s, classification after Bisdom et al., 1993) superficial horizons were found in the boreal forests of Canada (subartic continental climates) under conifer vegetation (Elmes et al., 2019). In the soils of BOR and HEL environments, the expression of WR can be linked to the abundance of OM coupled with low amounts of mineral surfaces (sand in Fig. 2a and total pedogenic Fe oxides in Table 1). Still, Fe oxides comprise a relatively high proportion of poorly crystalline forms (Fe_{OXA}/Fe_{DCB}, Table 1), which typically bear a larger specific surface area (Cornell and Schwertmann, 2003). It is reasonable to suppose that OM contents were sufficiently high to cover the larger surface area of these minerals. The BOR and HEL soils were also characterized by intermediate-to-low AS values, ca. 70 %, in line with published aggregate stability data of soils of other subalpine ecosystems (Girona-García et al., 2018), and a high RA. This implies that despite the presence of many RA, their contribution to the total amount of aggregates is limited (respect to other biomes). To explain it, we should consider that the low pH of these soils does not favor the interactions between Fe oxides (positively charged) and layer silicates, less negatively charged than at higher pH (Dixon et al., 1990).

On the opposite, TRO samples displayed extremely high AS values, that were not matched with a similarly high RA (Fig. 4d and g). This indicates that few aggregates were present, but still the proportion of resistant aggregates to the total amount of aggregates (AS) was high. The WR of TRO soils was moderate and, similarly, soils collected in a humid subtropical region in Brazil (A horizons) were testified to be slightly hydrophobic (Vogelmann et al., 2010). This suggests that, in the Tropical environment, the surfaces of Fe oxides (albeit highly crystalline, Table 1) are not fully saturated by OM adsorption, and can therefore easily enter in contact with water molecules. This occurs despite the abundance of sand-sized particles in the samples (Fig. 2a), many of whom are likely composed of Fe oxides (high $Fe_{DCB\ M}$, Fig. 3b).

The interaction between OM and mineral phases was further complicated by the multiplicity of binding agents coexisting in some of the soils (reflected in the remarkable differences in aggregate stability among biomes, Fig. 4d). In particular, aggregates can either develop hierarchically or not. In the former case, organic binding agents are involved, and the breakdown of macroaggregates originates smaller aggregates of variable dimensions (Legout et al., 2005). In the latter case (non-hierarchical structure), inorganic cements are mostly involved (Waters and Oades, 1991). As such, in presence of hierarchy, macroaggregates are typically OC-richer than microaggregates. In our dataset, the OC distribution in MACRO and MICRO indicates that aggregates are hierarchically structured (according to Six et al., 2000) in HEL, BOR and MED soils (Fig. 3a). In TRO soils, the low OC_M/OC_m points at a lack of hierarchy, in agreement with abundant Fe_{DCB} contents (Table 1 and Fig. 3b).

Based on the analyses, we then expected to see the synergic action of several inorganic binding agents in MED and TEM soils, where the contribution of carbonates, clay minerals and pedogenic Fe oxides was greater than in the other environments (Fig. 2 and Table 1). Carbonates are known to increase soil aggregation (Tisdall and Oades, 1982), but their role was here little visible as the soils where IC was present (MED and TEM, Fig. 2b) were also characterized by abundant OC contents. We nevertheless found significant correlations between IC and IC_M and abundance of the MACRO fraction ($R>0.400$, $p < 0.05$ at all Ts), and lower correlations with AS ($R < 0.300$, $p > 0.05$ at all Ts). This may suggest that IC promotes aggregate formation, but it is not directly related to the resistance of the aggregates. As IC was found both in MED and in TEM soils, the origin of the carbonates is likely both lithogenic and pedogenic. The importance of calcium as an aggregating agent −through the formation of cation bridges- has been largely demonstrated (Bertrand et al., 2007). However, the resistance of aggregates is significantly improved only when surface coating and pore infilling occur during the precipitation of pedogenic carbonates (Falsone et al., 2010).

Regarding the other two inorganic binding agents, existing studies testified a direct relationship between clay content and aggregate stability (Thomaz, 2021), and the positive influence of Fe and Al oxides on soil aggregation (Amézketa, 1999; Tisdall and Oades, 1982). Poorly crystalline oxides are particularly involved in forming stable bonds between soil particles (Duiker et al., 2003). However, different Fe pools seems to affect the abundance of RA and the proportion of RA to total soil aggregates (AS). When Fe pools are characterized by the prevalence of poorly crystalline forms, as in BOR, the abundance of resistant aggregates is favored (Fig. 4g). Yet, it is only in presence of high contents of Fe_{DCB} (TEM, MED and TRO soils, Table 1) that a stable aggregation is formed (Fig. 4d).

At last, SAV soils were dominated by sands like HEL and TRO (Fig. 2a), and the low availability of mineral surfaces was coupled with the absolute lowest OM contents. The low WR and AS values reflect the scarce association between these phases in SAV soils.

4.2. Effects of heating

Changes in OC, C/N, and pH were visible in all soils when temperatures raised above 200 °C (Table 1), indicating that OM is sensitive to fire in all biomes.. A remarkable decrease in OC content has frequently been reported in burnt superficial soil horizons (Mataix-Solera et al., 2002) for Ts greater than 200–250 °C (Badìa and Martì, 2003; Santín and Doerr, 2016), and the decrease in the C/N ratio was likely the consequence of the concentration of heat-resistant N-rich organic structures (Mastrolonardo et al., 2015). The increase in pH we observed has also been documented in other cases of heated soils (Glaser et al., 2002).

The distribution of aggregates in MACRO and MICRO did not significantly change with rising Ts, despite an increase in microaggregates has been documented after high-severity fires (Andreu

et al., 2001; Varela et al., 2010). Possibly, the lab heating treatment at 300 °C was not sufficient to cause a visible decrease of the MACRO fraction. Indeed, heat altered the OC contents of MACRO and MICRO fractions (Fig. 3c), with higher proportional OC losses in MACRO. Non-homogeneous OC losses among soil size fractions have been reported also in the literature (Nocentini et al., 2010). On this regard, it is generally accepted that a higher OM protection (by stabilization) is guaranteed by minerals in the MICRO fraction (Stewart et al., 2009; Zimmermann et al., 2007). Since N-rich organic moieties can be fairly resistant to heat (Knicker, 2007), the lower C/N of the MICRO fraction might play a role in limiting OC losses. This ratio cannot however explain the differences among biomes visible in Fig. 3d, as the lower-most proportional OC losses were recorded in case of the MED MACRO fraction. Likely, OC losses were in this case limited by the high clay content of MED soils (Fig. 2a), as the fundamental protection exerted by clay-sized minerals has extensively been documented (Kiem and Kögel-Knabner, 2002; Six et al., 2002; Watts et al., 2005).

Increase in soil water repellency with heat was expected to occur in the temperature-range we selected (DeBano, 2000a), and we observed it at 200 °C for those soils that were hydrophobic already at RT (HEL and BOR biomes, Fig. 4a). As discussed in the previous section (4.1), HEL and BOR soils were characterized by a low surface area and consistent OM contents, and probably the soils of the other biomes did not display a heat-induced WR build-up as a result of the scattered distribution of organic compounds onto mineral surfaces (Kaiser and Guggenberger, 2003). The development of soil WR at high Ts can influence the behavior of aggregates, since hydrophobic coatings can make aggregates less susceptible to water breakdown (Ellerbrock and Gerke, 2004; Fox et al., 2007; Terefe et al., 2008). According to the conceptual model proposed by Mataix-Solera et al. (2011), in fact, hydrophobic soils possessing OM as the main binding agent are expected to show an increase in AS for intermediate fire severities, with a sharp decrease in AS for high severities. We therefore expected a loss of aggregation upon severe heating in the soils of biomes where organic binding agents dominated (based on aggregate hierarchy: HEL, BOR, and MED to some extent) and where soils possessed a clear hydrophobic character (HEL and BOR). Since the MED soils did not experience WR build-up, and since AS of MED soils reached its maximum after 200 °C (Fig. 4f), the involvement of multiple cementing agents in these soils was again confirmed. Overall, in TRO soils there was no change in water repellency (Fig. 4a and 4b) and aggregate stability (Fig. 4d to 4f), possibly because of the paucity of OM and the higher temperatures needed to significantly affect the structure −and aggregating potential- of crystalline Fe forms (Cornell and Schwertmann, 2003). The SAV soils were unaffected in terms of infiltration times. Similarly, other savannah soils of North-Eastern South Africa (Kruger National Park, with a hot semi-arid climate) were documented be wettable after fire occurrence (Strydom et al., 2019). As for aggregation, the increase in AS and RA with heating in SAV samples is somewhat puzzling. These soils do not contain IC, have low OC and Fe oxides contents, but might still have experienced small rearrangements in the poor interaction between OM and minerals.

At 300 °C, the loss of hydrophobicity occurred in all the soils (Fig. 4c). In the literature, due to the absence of a uniform protocol, more than one T-threshold has been found to demark WR loss. Temperatures of 280–400 °C (Doerr et al., 2005), 270–300 °C (Atanassova and Doerr, 2011; García-Corona et al., 2004; Zavala et al., 2010) or 225 °C (Simkovic et al., 2008) have been identified. Nevertheless, when an analogue heating experiment was performed on soils developed in the North-Western Italian Alps (Negri et al., 2021), a drastic decrease of infiltration times was similarly detected at 300 °C. According to the most widely accepted explanation, this occurs due to the destruction of the organic compounds responsible for the coating of mineral surfaces (DeBano, 2000a). The soils showing the biggest changes in water repellency between RT and 300 °C were those belonging to the BOR and HEL biomes (Fig. 4a and 4c), that lost a high proportion of OC with respect to the initial condition (Fig. S1), but share the disappearance of WR with the soils from all the other biomes. The mere transformations in OM compounds are therefore not able to explain such variations in the soil WR behavior, and it is thus fundamental to consider the interaction with the mineral phase.

4.3. Drivers of extreme WR and AS loss

Soil OC content was expected to be among the top factors with explanatory power in WR expression, given its renowned relevance (Doerr et al., 2000). The low ranking of OC in the RF model (Fig. 6a) suggests that the OC-WR relationship is heavily influenced by OM composition and transformations occurring upon burning (Jiménez-Morillo et al., 2022) and, also, these dynamics are equally ruled by organo-mineral interactions (availability of mineral surfaces: clay, sand, fine silt contents, and Fe oxides, as visible in Fig. 6a). Still, the often-cited importance of mineral surfaces of low surface area (Scott, 2000) was less important in discriminating the soils with extreme WR (Fig. S3a) than biome-related indexes, such as the AI and the relative proportion of poorly crystalline oxides (Fig. 6). This is likely caused by the abundance of sand fractions in biomes that showed an opposite behavior in terms of water repellency (HEL and BOR *vs.* TRO and SAV). From these results, neither the OC content nor the texture can be used to predict WR in all world biomes. Instead, a biome-specific behavior has to be expected. Also, a greater incidence of extreme WR is expected for soils developed under conifer vegetation (Negri et al., 2021; Zavala et al., 2014). This did not emerge (Fig. S4a), possibly because conifer vegetation characterized different biomes (Table S1) which displayed very different WR tendencies (Fig. 4a and b).

Looking at the outputs of the first RF model in relation to the climatic factor, we then have to remember that high erosion yields often follow wildfires (Certini, 2005; Moody et al., 2013) primarily in dependence of topography (Smith et al., 2011), and frequency and severity of the disturbance (Shakesby and Doerr, 2006). Therefore, mountain areas characterized by high AI values could not only develop extreme WR, but may also originate consistent erosion.

Regarding aggregation, the complexity of the mechanisms involved is likely responsible for the lack of a clear discrimination between soils that did or did not experience loss of aggregate stability upon rising temperatures (Fig. S3b). The importance of the MACRO fraction abundance in describing resistance of aggregates (Fig. 7a, b) confirms this hypothesis. It suggests that the same soil properties responsible for MACRO aggregates formation are also fundamental in ruling the strength of the aggregates. Even in this case, a biome-related specificity was noted. The most sensitive soils were either those in cold areas or where high precipitation occurs (AI>70). Similarly, AS was documented to be lower in fire-affected areas located in high-elevation Alpine regions (Vacchiano et al., 2014), while a greater AS was found in MED soils subjected either to rising Ts (Guerrero et al., 2001) or fire occurrence (Arcenegui et al., 2008). Among others, the effect of crystalline and poorly-ordered Fe oxides that has vastly been established in the literature (Barthès et al., 2008) here emerged (3rd partial dependence plot in Fig. 7b) over that of IC (7th factor in Fig. 7a).

5. Conclusions

Soil WR was highly inhomogeneous in the various biomes, and peaked at 200 °C in samples belonging to High elevation/latitudes ecosystems and Boreal forests. In all cases, WR disappeared for Ts > 200 °C. Soil AS was also highly variable: some samples displayed a decrease in AS with rising Ts, while others showed an increase.

The first RF model evidenced that acidic soils (pH<7) developed in regions with high aridity index (AI) values (AI>75) are prone to experiencing extreme WR at 200 °C. Also, low clay contents (<10 %) and a low crystallinity of Fe oxides (Fe_{OXA}/Fe_{DCB}>40 %) were among the first explanatory factors responsible for high WR, and thus Entisols, Inceptisols, Spodosols and Alfisols of either high latitude or altitude

ecosystems are expected to develop extreme WR after the passage of a fire of moderate intensity.

The rising Ts did not cause a decrease in AS in well-developed soils of Mediterranean and Tropical forests, and in Savannah. According to the second RF model, sites with low-moderate AI values (<70), and where aggregation is ruled by moderate OM contents (ca. 50 g kg^{-1} of OC) and abundant clay and Fe oxyhydroxides, are less prone to experience AS loss up to 300 °C. As such, even considering a flat-topography scenario, soils developed under cold climates appear as extremely susceptible to disaggregation. Many mountain areas where these soils are present are characterized by steep slopes, which may constitute a further predisposing factor for high erosion yields.

We hope a larger dataset of topsoils will be subjected to the similar investigations, so as to create robust model able to predict the behavior of soils starting from their properties and localization. Adding up to this level of complexity, it is known that natural and fire-affected WR and AS are not static in time, and present inter-annual seasonal variability. These phenomena need to be further tackled and understood so as to direct the attention and resources to those environments which are less resilient to fire occurrence, or might be in the future due to the action of climate change.

Funding sources

This work was funded by the Compagnia di San Paolo in the framework of the project *Alterations of soil physico-chemical properties as a consequence of forest fires* (UNITO S1921 EX-POST).

CRediT authorship contribution statement

S. Negri: Writing – review & editing, Writing – original draft, Visualization, Validation, Methodology, Investigation, Formal analysis, Data curation, Conceptualization. **V. Arcenegui:** Writing – review & editing, Supervision, Methodology, Investigation, Formal analysis, Conceptualization. **J. Mataix-Solera:** Writing – review & editing, Validation, Supervision, Investigation, Conceptualization. **E. Bonifacio:** Writing – review & editing, Validation, Supervision, Resources, Project administration, Investigation, Data curation, Conceptualization.

Declaration of competing interest

The authors declare that they have no known competing financial interests or personal relationships that could have appeared to influence the work reported in this paper.

Data availability

Data will be made available on request.

Acknowledgments

We sincerely thank Giacomo Certini for reviewing the Doctoral thesis from which this article was produced. We also thank Ana Perez Gimeno for assistance during AAS measurements. We would also thank Débora Rodrigues Rocha and Yasmin Tadeu Costa for having supplied the two samples from Brazil.

Appendix A. Supplementary data

Supplementary data to this article can be found online at https://doi.org/10.1016/j.catena.2024.108257.

References

Amézketa, E., 1999. Soil aggregate stability: a review. J. Sustain. Agric. 14 (2–3), 83–151.
Andrés-Abellán, M., Wic-Baena, C., López-Serrano, F.R., García-Morote, F.A., Martínez-García, E., Picazo, M.I., Rubio, E., Moreno-Ortego, J.L., Bastida-López, F., García-Izquierdo, C., 2019. A soil-quality index for soil from Mediterranean forests. Eur. J. Soil Sci. 70 (5), 1001–1011.
Andreu, V., Imeson, A.C., Rubio, J.L., 2001. Temporal changes in soil aggregates and water erosion after a wildfire in a Mediterranean pine forest. Catena 44 (1), 69–84.
Araya, S.N., Meding, M., Berhe, A.A., 2016. Thermal alteration of soil physico-chemical properties: a systematic study to infer response of Sierra Nevada climosequence soils to forest fires. Soil 2 (3), 351–366.
Araya, S.N., Fogel, M.L., Berhe, A.A., 2017. Thermal alteration of soil organic matter properties: a systematic study to infer response of Sierra Nevada climosequence soils to forest fires. Soil 3 (1), 31.
Arcenegui, V., Mataix-Solera, J., Guerrero, C., Zornoza, R., Mayoral, A.M., Morales, J., 2007. Factors controlling the water repellency induced by fire in calcareous Mediterranean forest soils. Eur. J. Soil Sci. 58 (6), 1254–1259.
Arcenegui, V., Mataix-Solera, J., Guerrero, C., Zornoza, R., Mataix-Beneyto, J., García-Orenes, F., 2008. Immediate effects of wildfires on water repellency and aggregate stability in Mediterranean calcareous soils. Catena 74 (3), 219–226.
Artés, T., Oom, D., De Rigo, D., Durrant, T.H., Maianti, P., Libertà, G., San-Miguel-Ayanz, J., 2019. A global wildfire dataset for the analysis of fire regimes and fire behaviour. Sci. Data 6 (1), 296.
Atanassova, I., Doerr, S.H., 2011. Changes in soil organic compound composition associated with heat-induced increases in soil water repellency. Eur. J. Soil Sci. 62 (4), 516–532.
Badìa, D., Martì, C., 2003. Plant ash and heat intensity effects on chemical and physical properties of two contrasting soils. Arid Land Res. Manag. 17 (1), 23–41.
Badía-Villas, D., González-Pérez, J.A., Aznar, J.M., Arjona-Gracia, B., Martí-Dalmau, C., 2014. Changes in water repellency, aggregation and organic matter of a mollic horizon burned in laboratory: Soil depth affected by fire. Geoderma 213, 400–407.
Barthès, B.G., Kouakoua, E., Larré-Larrouy, M.-C., Razafimbelo, T.M., de Luca, E.F., Azontonde, A., Neves, C.S.V.J., de Freitas, P.L., Feller, C.L., 2008. Texture and sesquioxide effects on water-stable aggregates and organic matter in some tropical soils. Geoderma 143 (1–2), 14–25.
Beatty, S.M., Smith, J.E., 2010. Fractional wettability and contact angle dynamics in burned water repellent soils. J. Hydrol. 391 (1–2), 97–108.
Bertrand, I., Delfosse, O., Mary, B., 2007. Carbon and nitrogen mineralization in acidic, limed and calcareous agricultural soils: apparent and actual effects. Soil Biol. Biochem. 39 (1), 276–288.
Bisdom, E.B.A., Dekker, L.W., Schoute, J.F.T., 1993. Water repellency of sieve fractions from sandy soils and relationships with organic material and soil structure. In: Soil Structure/soil Biota Interrelationships. Elsevier, pp. 105–118.
Bonifacio, E., Santoni, S., Falsone, G., Zanini, E., 2006. Wet aggregate stability of some Botswana soil profiles. Arid Land Res. Manag. 20 (1), 15–28.
Bonifacio, E., Falsone, G., Simonov, G., Sokolova, T., Tolpeshta, I., 2009. Pedogenic processes and clay transformations in bisequal soils of the Southern Taiga zone. Geoderma 149 (1–2), 66–75.
Borggaard, O.K., 1985. Organic matter and silicon in relation to the crystallinity of soil iron oxides. Acta Agric. Scand. 35 (4), 398–406.
Bowman, D.M.J.S., Balch, J.K., Artaxo, P., Bond, W.J., Carlson, J.M., Cochrane, M.A., D'Antonio, C.M., DeFries, R.S., Doyle, J.C., Harrison, S.P., Johnston, F.H., Keeley, J. E., Krawchuk, M., Kull, C.A., Marston, J.B., Moritz, M.A., Prentice, I.C., Roos, C.I., Scott, A.C., Swetnam, T.W., van der Werf, G., Pyne, S.J., 2009. Fire in the Earth system. Science 324 (5926), 481–484.
Bowman, D.J.S., Kolden, C., Abatzoglou, J.T., van der Werf, G.R., Flannigan, M., 2020. Vegetation fires in the Anthropocene. Nature Rev. Earth Environ. 1 (10), 500–515.
Breiman, L., 2001. Random forests. Mach. Learn. 45, 5–32.
Caballero, R., Fernandez-Gonzalez, F., Badia, R.P., Molle, G., Roggero, P.P., Bagella, S., Papanastasis, V.P., Fotiadis, G., Sidiropoulou, A., Ispikoudis, I., et al., 2011. Grazing systems and biodiversity in Mediterranean areas: Spain Italy and Greece. Pastos 39 (1), 9–154.
Catoni, M., D'Amico, M.E., Zanini, E., Bonifacio, E., 2016. Effect of pedogenic processes and formation factors on organic matter stabilization in alpine forest soils. Geoderma 263, 151–160.
Certini, G., 2005. Effects of fire on properties of forest soils: a review. Oecologia 143 (1), 1–10.
Chen, Y., Romps, D.M., Seeley, J.T., Veraverbeke, S., Riley, W.J., Mekonnen, Z.A., Randerson, J.T., 2021. Future increases in Arctic lightning and fire risk for permafrost carbon. Nat. Clim. Chang. 11 (5), 404–410.
Cornell, R., Schwertmann, U., 2003. The iron oxides: structure, properties, reactions, occurrences and uses. John Wiley & Sons.
De Martonne, E., 1926. Aréisme et Indice d'aridité. Comptes Rendus de L'Academy of Science, Paris, pp. 1395–1398.
DeBano, L.F., 2000a. The role of fire and soil heating on water repellency in wildland environments: a review. J. Hydrol. 231, 195–206.
DeBano, L.F., 2000b. Water repellency in soils: a historical overview. J. Hydrol. 231 (232), 4–32.
Diehl, D., Bayer, J.V., Woche, S.K., Bryant, R., Doerr, S.H., Schaumann, G.E., 2010. Reaction of soil water repellency to artificially induced changes in soil pH. Geoderma 158 (3–4), 375–384.
Dixon, J.B., Weed, S.B., Parpitt, R.L., 1990. Minerals in soil environments. Soil Sci. 150 (2), 562.
Doerr, S.H., Shakesby, R.A., Walsh, R.P.D., 2000. Soil water repellency: its causes, characteristics and hydro-geomorphological significance. Earth Sci. Rev. 51 (1–4), 33–65.
Doerr, S.H., Llewellyn, C.T., Douglas, P., Morley, C.P., Mainwaring, K.A., Haskins, C., Johnsey, L., Ritsema, C.J., Stagnitti, F., Allinson, G., 2005. Extraction of compounds

associated with water repellency in sandy soils of different origin. Soil Res. 43 (3), 225–237.
Duiker, S.W., Rhoton, F.E., Torrent, J., Smeck, N.E., Lal, R., 2003. Iron (hydr) oxide crystallinity effects on soil aggregation. Soil Sci. Soc. Am. J. 67 (2), 606–611.
Ehrlinger, J. (2016). ggRandomForests: Exploring random forest survival. *ArXiv Preprint ArXiv:1612.08974*.
Ellerbrock, R.H., Gerke, H.H., 2004. Characterizing organic matter of soil aggregate coatings and biopores by Fourier transform infrared spectroscopy. Eur. J. Soil Sci. 55 (2), 219–228.
Elmes, M.C., Thompson, D.K., Price, J.S., 2019. Changes to the hydrophysical properties of upland and riparian soils in a burned fen watershed in the Athabasca Oil Sands Region, northern Alberta Canada. Catena 181, 104077.
Falsone, G., Catoni, M., Bonifacio, E., 2010. Effects of calcite on the soil porous structure: natural and experimental conditions. Agrochimica 54 (1), 1–12.
Falsone, G., Bonifacio, E., Zanini, E., 2012. Structure development in aggregates of poorly developed soils through the analysis of the pore system. Catena 95, 169–176.
FAO. (2020). *Global Forest Resources Assessment. Main report.* 165.
Fedotov, G.N., Tretyakov, Y.D., Dobrovolskii, G.V., Putlyaev, V.I., Pakhomov, E.I., Fankovskaya, A.A., Pochatkova, T.N., 2006. Water resistance of soil aggregates and gel structures. Dokl. Chem. 411 (1), 215–218.
Ferreira, A.J.D., Coelho, C.O.A., Boulet, A.K., Leighton-Boyce, G., Keizer, J.J., Ritsema, C. J., 2005. Influence of burning intensity on water repellency and hydrological processes at forest and shrub sites in Portugal. Soil Res. 43 (3), 327–336.
Fox, D.M., Darboux, F., Carrega, P., 2007. Effects of fire-induced water repellency on soil aggregate stability, splash erosion, and saturated hydraulic conductivity for different size fractions. Hydrol. Process. 21 (17), 2377–2384.
García-Corona, R., Benito, E., De Blas, E., Varela, M.E., 2004. Effects of heating on some soil physical properties related to its hydrological behaviour in two north-western Spanish soils. Int. J. Wildland Fire 13 (2), 195–199.
Gee, G.W., Bauder, J.W., 1986. Particle-size analysis. Methods of Soil Analysis: Part 1 Physical and Mineralogical Methods 5, 383–411.
Gee, G.W., Or, D., 2002. 2.4 Particle-size analysis. Methods of Soil Analysis: Part 4 Physical Methods 5, 255–293.
Giovannini, G., Lucchesi, S., 1997. Modifications induced in soil physico-chemical parameters by experimental fires at different intensities. Soil Sci. 162 (7), 479–486.
Girona-García, A., Ortiz-Perpiñá, O., Badía-Villas, D., Dalmau, C., 2018. Effects of prescribed burning on soil organic C, aggregate stability and water repellency in a subalpine shrubland: Variations among sieve fractions and depths. Catena 166, 68–77.
Glaser, B., Lehmann, J., Zech, W., 2002. Ameliorating physical and chemical properties of highly weathered soils in the tropics with charcoal–a review. Biol. Fertil. Soils 35 (4), 219–230.
Glasspool, I.J., Scott, A.C., Waltham, D., Pronina, N.V., Shao, L., 2015. The impact of fire on the Late Paleozoic Earth system. Front. Plant Sci. 6, 756.
Guerrero, C., Mataix-Solera, J., Navarro-Pedreño, J., García-Orenes, F., Gómez, I., 2001. Different patterns of aggregate stability in burned and restored soils. Arid Land Res. Manag. 15 (2), 163–171.
Harris, D., Horwáth, W.R., Van Kessel, C., 2001. Acid fumigation of soils to remove carbonates prior to total organic carbon or carbon-13 isotopic analysis. Soil Sci. Soc. Am. J. 65 (6), 1853–1856.
Hilli, S., Stark, S., Derome, J., 2010. Litter decomposition rates in relation to litter stocks in boreal coniferous forests along climatic and soil fertility gradients. Appl. Soil Ecol. 46 (2), 200–208.
Hubbert, K.R., Preisler, H.K., Wohlgemuth, P.M., Graham, R.C., Narog, M.G., 2006. Prescribed burning effects on soil physical properties and soil water repellency in a steep chaparral watershed, southern California, USA. Geoderma 130 (3–4), 284–298.
Janzen, C., Tobin-Janzen, T., 2008. Microbial communities in fire-affected soils. In: Microbiology of Extreme Soils. Springer, pp. 299–316.
Jiménez-Morillo, N.T., Almendros, G., Miller, A.Z., Hatcher, P.G., González-Pérez, J.A., 2022. Hydrophobicity of soils affected by fires: An assessment using molecular markers from ultra-high resolution mass spectrometry. Sci. Total Environ. 817, 152957.
Jolly, W.M., Cochrane, M.A., Freeborn, P.H., Holden, Z.A., Brown, T.J., Williamson, G.J., Bowman, D.M., 2015. Climate-induced variations in global wildfire danger from 1979 to 2013. Nat. Commun. 6 (1), 1–11.
Jordán, A., Zavala, L.M., Mataix-Solera, J., Nava, A.L., Alanís, N., 2011. Effect of fire severity on water repellency and aggregate stability on Mexican volcanic soils. Catena 84 (3), 136–147.
Kaiser, K., Guggenberger, G., 2003. Mineral surfaces and soil organic matter. Eur. J. Soil Sci. 54 (2), 219–236.
Karger, D.N., Conrad, O., Böhner, J., Kawohl, T., Kreft, H., Soria-Auza, R.W., Zimmermann, N.E., Linder, P., Kessler, M., 2017. Climatologies at high resolution for the Earth land surface areas. Sci. Data 4, 170122. https://doi.org/10.1038/sdata.2017.122.
Kiem, R., Kögel-Knabner, I., 2002. Refractory organic carbon in particle-size fractions of arable soils II: organic carbon in relation to mineral surface area and iron oxides in fractions< 6 µm. Org Geochem. 33 (12), 1699–1713.
Knicker, H., 2007. How does fire affect the nature and stability of soil organic nitrogen and carbon? A Review. Biogeochemistry 85 (1), 91–118.
Komac, B., Kéfi, S., Nuche, P., Escós, J., Alados, C.L., 2013. Modeling shrub encroachment in subalpine grasslands under different environmental and management scenarios. J. Environ. Manage. 121, 160–169.
Legout, C., Leguédois, S., Le Bissonnais, Y., 2005. Aggregate breakdown dynamics under rainfall compared with aggregate stability measurements. Eur. J. Soil Sci. 56 (2), 225–238.
Llovet, J., Ruiz-Valera, M., Josa, R., Vallejo, V.R., 2009. Soil responses to fire in Mediterranean forest landscapes in relation to the previous stage of land abandonment. Int. J. Wildland Fire 18 (2), 222–232.
Loeppert R.H., I. W. P. (1996). *Iron - Methods of soil analysis, part 3: Chemical methods.* Madison, WI, USA.
Malkinson, D., Wittenberg, L., 2011. Post fire induced soil water repellency—Modeling short and long-term processes. Geomorphology 125 (1), 186–192.
Mantero, G., Morresi, D., Marzano, R., Motta, R., Mladenoff, D.J., Garbarino, M., 2020. The influence of land abandonment on forest disturbance regimes: a global review. Landsc. Ecol. 35 (12), 2723–2744.
Mastrolonardo, G., Rumpel, C., Forte, C., Doerr, S.H., Certini, G., 2015. Abundance and composition of free and aggregate-occluded carbohydrates and lignin in two forest soils as affected by wildfires of different severity. Geoderma 245, 40–51.
Mataix-Solera, J., Cerdà, A., Arcenegui, V., Jordán, A., Zavala, L.M., 2011. Fire effects on soil aggregation: a review. Earth Sci. Rev. 109 (1–2), 44–60.
Mataix-Solera, J., Arcenegui, V., Zavala, L.M., Pérez-Bejarano, A., Jordán, A., Morugán-Coronado, A., Bárcenas-Moreno, G., Jiménez-Pinilla, P., Lozano, E., Granged, A.J.P., Gil-Torres, J., 2014. Small variations of soil properties control fire-induced water repellency. Span. J. Soil Sci. 4, 51–60.
Mataix-Solera, J., Arellano, E.C., Jaña, J.E., Olivares, L., Guardiola, J., Arcenegui, V., García-Carmona, M., García-Franco, N., Valenzuela, P., 2021. Soil vulnerability indicators to degradation by wildfires in Torres del Paine National Park (Patagonia, Chile). Spanish J. Soil Sci. 11, 10008.
Mataix-Solera, J., Gómez, I., Navarro-Pedreño, J., Guerrero, C., Moral, R., 2002. Soil organic matter and aggregates affected by wildfire in a *Pinus halepensis* forest in a Mediterranean environment. Int. J. Wildland Fire 11 (2), 107–114.
Mehra, O.P., Jackson, M.L., 1958. Iron oxide removal from soils and clays by a dithionite–citrate system buffered with sodium bicarbonate. In: Clays and Clay Minerals. Elsevier, pp. 317–327.
Merino, A., Fonturbel, M.T., Fernández, C., Chávez-Vergara, B., García-Oliva, F., Vega, J. A., 2018. Inferring changes in soil organic matter in post-wildfire soil burn severity levels in a temperate climate. Sci. Total Environ. 627, 622–632.
Moody, J.A., Shakesby, R.A., Robichaud, P.R., Cannon, S.H., Martin, D.A., 2013. Current research issues related to post-wildfire runoff and erosion processes. Earth Sci. Rev. 122, 10–37.
Negri, S., Stanchi, S., Celi, L., Bonifacio, E., 2021. Simulating wildfires with lab-heating experiments: Drivers and mechanisms of water repellency in alpine soils. Geoderma 402, 115357.
Nocentini, C., Certini, G., Knicker, H., Francioso, O., Rumpel, C., 2010. Nature and reactivity of charcoal produced and added to soil during wildfire are particle-size dependent. Org Geochem. 41 (7), 682–689.
Papierowska, E., Matysiak, W., Szatyłowicz, J., Debaene, G., Urbanek, E., Kalisz, B., Łachacz, A., 2018. Compatibility of methods used for soil water repellency determination for organic and organo-mineral soils. Geoderma 314, 221–231.
Pellegrini, A.F.A., Harden, J., Georgiou, K., Hemes, K.S., Malhotra, A., Nolan, C.J., Jackson, R.B., 2022. Fire effects on the persistence of soil organic matter and long-term carbon storage. Nat. Geosci. 15 (1), 5–13.
Pickett, S.T.A., White, P.S., 2013. The ecology of natural disturbance and patch dynamics. Elsevier.
Roldán, A., Albaladejo, J., Thornes, J.B., 1996. Aggregate stability changes in a semiarid soil after treatment with different organic amendments. Arid Land Res. Manag. 10 (2), 139–148.
Santín, C., Doerr, S.H., 2016. Fire effects on soils: the human dimension. Philos. Trans. R. Soc., B 371 (1696), 20150171.
Schwertmann, U., 1964. Differenzierung der Eisenoxide des Bodens durch photochemische Extraktion mit saurer Ammoniumoxalat-Lösung. Zeischrift Für Pflanzenernährung, Düngung Und Bodenkunde 202, 105–194.
Scott, D.F., 2000. Soil wettability in forested catchments in South Africa; as measured by different methods and as affected by vegetation cover and soil characteristics. J. Hydrol. 231, 87–104.
Shakesby, R.A., Doerr, S.H., 2006. Wildfire as a hydrological and geomorphological agent. Earth Sci. Rev. 74 (3–4), 269–307.
Simkovic, I., Dlapa, P., Doerr, S.H., Mataix-Solera, J., Sasinkova, V., 2008. Thermal destruction of soil water repellency and associated changes to soil organic matter as observed by FTIR spectroscopy. Catena 74 (3), 205–211.
Six, J., Paustian, K., Elliott, E.T., Combrink, C., 2000. Soil structure and organic matter I. Distribution of aggregate-size classes and aggregate-associated carbon. Soil Sci. Soc. Am. J. 64 (2), 681–689.
Six, J., Feller, C., Denef, K., Ogle, S., de Moraes Sa, J.C., Albrecht, A., 2002. Soil organic matter, biota and aggregation in temperate and tropical soils-Effects of no-tillage. Agronomie 22 (7–8), 755–775.
Smith, H.G., Sheridan, G.J., Lane, P.N.J., Nyman, P., Haydon, S., 2011. Wildfire effects on water quality in forest catchments: A review with implications for water supply. J. Hydrol. 396 (1–2), 170–192.
Soil Survey Staff, 1999. Soil taxonomy: A basic system of soil classification for making and interpreting soil surveys, second ed. Natural Resources Conservation Service. U. S Department of Agriculture Handbook, p. 436.
Stewart, C.E., Paustian, K., Conant, R.T., Plante, A.F., Six, J., 2009. Soil carbon saturation: Implications for measurable carbon pool dynamics in long-term incubations. Soil Biol. Biochem. 41 (2), 357–366.
Strydom, T., Riddell, E.S., Rowe, T., Govender, N., Lorentz, S.A., le Roux, P.A.L., Wigley-Coetsee, C., 2019. The effect of experimental fires on soil hydrology and nutrients in an African savanna. Geoderma 345, 114–122.
Terefe, T., Mariscal-Sancho, I., Peregrina, F., Espejo, R., 2008. Influence of heating on various properties of six Mediterranean soils A Laboratory Study. Geoderma 143 (3–4), 273–280.

Thomaz, E.L., 2021. Effects of fire on the aggregate stability of clayey soils: A meta-analysis. Earth Sci. Rev. 221, 103802.
Tisdall, J.M., Oades, J.M., 1982. Organic matter and water-stable aggregates in soils. J. Soil Sci. 33 (2), 141–163.
Vacchiano, G., Stanchi, S., Marinari, G., Ascoli, D., Zanini, E., Motta, R., 2014. Fire severity, residuals and soil legacies affect regeneration of Scots pine in the Southern Alps. Sci. Total Environ. 472, 778–788.
Varela, M.E., Benito, E., Keizer, J.J., 2010. Effects of wildfire and laboratory heating on soil aggregate stability of pine forests in Galicia: The role of lithology, soil organic matter content and water repellency. Catena 83 (2–3), 127–134.
Vogelmann, E.S., Reichert, J.M., Reinert, D.J., Mentges, M.I., Vieira, D.A., de Barros, C.A. P., Fasinmirin, J.T., 2010. Water repellency in soils of humid subtropical climate of Rio Grande do Sul Brazil. Soil Tillage Res. 110 (1), 126–133.
Waters, A. G., Oades, J. M. (1991). Organic matter in water-stable aggregates. *Advances in Soil Organic Matter Research: The Impact on Agriculture and the Environment*, *90*, 163–174.
Watts, C.W., Whalley, W.R., Brookes, P.C., Devonshire, B.J., Whitmore, A.P., 2005. Biological and physical processes that mediate micro-aggregation of clays. Soil Sci. 170 (8), 573–583.
Zavala, L.M., Granged, A.J.P., Jordán, A., Bárcenas-Moreno, G., 2010. Effect of burning temperature on water repellency and aggregate stability in forest soils under laboratory conditions. Geoderma 158 (3–4), 366–374.
Zavala, L.M., García-Moreno, J., Gordillo-Rivero, Á.J., Jordán, A., Mataix-Solera, J., 2014. Natural soil water repellency in different types of Mediterranean woodlands. Geoderma 226, 170–178.
Zimmermann, M., Leifeld, J., Schmidt, M.W.I., Smith, P., Fuhrer, J., 2007. Measured soil organic matter fractions can be related to pools in the RothC model. Eur. J. Soil Sci. 58 (3), 658–667.